Am J Physiol Heart Circ Physiol 293: H660–H669, 2007.
First published January 12, 2007; doi:10.1152/ajpheart.01083.2006.

Frequency-dependent effects of various I_{Kr} blockers on cardiac action potential duration in a human atrial model

Kenji Tsujimae,[1] Shingo Suzuki,[1] Shingo Murakami,[1] and Yoshihisa Kurachi[1,2]

[1]*Division of Molecular and Cellular Pharmacology, Department of Pharmacology, Graduate School of Medicine, and* [2]*Center for Advanced Medical Engineering and Informatics, Osaka University, Osaka, Japan*

Submitted 4 October 2006; accepted in final form 6 January 2007

Tsujimae K, Suzuki S, Murakami S, Kurachi Y. Frequency-dependent effects of various I_{Kr} blockers on cardiac action potential duration in a human atrial model. *Am J Physiol Heart Circ Physiol* 293: H660–H669, 2007. First published January 12, 2007; doi:10.1152/ajpheart.01083.2006.—Rapidly activating K^+ current (I_{Kr}) blockers prolong action potential (AP) duration (APD) in a reverse-frequency-dependent manner and may induce arrhythmias, including torsade de pointes in the ventricle. The I_{Kr} blocker dofetilide has been approved for treatment of atrial arrhythmias, including fibrillation. There are, however, a limited number of studies on the action of I_{Kr} blockers on atrial AP. When we tested a mathematical model of the human atrial AP (M Courtemanche, RJ Ramirez, S Nattel. *Am J Physiol Heart Circ Physiol* 275: H301–H321, 1998) to examine the effects of dofetilide-type I_{Kr} blockade, this model could not reproduce the reverse-frequency-dependent nature of I_{Kr} blockade on atrial APD. We modified the model by introducing a slowly activating K^+ current activation parameter. As the slow time constant was increased, dofetilide-type blockade induced more prominent reverse-frequency-dependent APD prolongation. Using the modified model, we also examined the effects of two more types of I_{Kr} blockade similar to those of quinidine and vesnarinone. Voltage- and time-dependent block of I_{Kr} through the onset of inhibition by quinidine is much faster than by vesnarinone. When we incorporated the kinetics of the effects of these drugs on I_{Kr} into the model, we found that quinidine-type blockade caused a reverse-frequency-dependent prolongation of APD that was similar to the effect of dofetilide-type blockade, whereas vesnarinone-type blockade did not. This finding coincides with experimental observations. The lack of the reverse frequency dependence in vesnarinone-type blockade was accounted for by the slow development of I_{Kr} blockade at depolarized potentials. These results suggest that the voltage- and time-dependent nature of I_{Kr} blockade by drugs may be critical for the phenotype of the drug effect on atrial AP.

rapidly activating potassium current; slowly activating potassium current; atrial action potential; reverse frequency dependence; computer simulation

THE DELAYED RECTIFIER K^+ current (I_K) contributes to the phase 2 and phase 3 repolarization of the cardiac action potential (AP) and, thus, controls AP duration (APD). The rapidly activating K^+ current (I_{Kr}) and the slowly activating K^+ current (I_{Ks}) are two distinct components of I_K in many mammals, including humans (28, 29, 37). I_{Kr} inhibition by a number of cardiac and noncardiac drugs prolongs the QT interval and causes arrhythmias, including torsades de pointes in the ventricle (1). The contribution of I_{Kr} relative to I_{Ks} in AP repolarization is greater during bradycardia than during tachycardia: during tachycardia, the amplitude of I_{Ks} increases because of its slow deactivation, whereas the amplitude of I_{Kr} remains nearly the same (12). As a result, drugs such as dofetilide and E-4031, which specifically inhibit I_{Kr}, prolong APD more prominently during bradycardia (17, 18, 32). This phenomenon is called "reverse frequency dependence." The reverse-frequency-dependent nature of a drug's effect is considered, at least in part, to be responsible for inducing excessive prolongation of APD and torsades de pointes during bradycardia (11). It is a critical indicator of the arrhythmogenic potential of a drug (34).

Drugs such as dofetilide and E-4031 block I_{Kr} in a voltage- and time-independent manner (32, 33). On the other hand, we showed that the positive inotropic agent vesnarinone and the widely used class Ia antiarrhythmic drug quinidine inhibit current flowing through the pore-forming subunit of I_{Kr}, HERG (human *ether-a-go-go*-related gene), in a voltage- and time-dependent manner (13, 33). Although both drugs inhibit the current more potently and rapidly as the membrane potential is depolarized, the development of blockade at the same potential is much faster with quinidine than with vesnarinone (13, 33). Accordingly, I_{Kr} blockade by drugs can be classified into at least three representative groups: voltage- and time-independent blockade (e.g., by dofetilide and E-4031), fast voltage- and time-dependent blockade (e.g., by quinidine), and slow voltage- and time-dependent blockade (e.g., by vesnarinone). Previous studies have shown that although dofetilide and quinidine cause reverse-frequency-dependent prolongation of APD, vesnarinone does not (10, 12, 32) and that, clinically, dofetilide and quinidine often cause torsades de pointes, but vesnarinone does not (7, 30). These different effects among the drugs may be due to the differences in their kinetics of HERG blockade (13, 33), but the underlying mechanism has not been fully clarified.

I_{Kr} and I_{Ks} were also found in human atrial myocytes (37), and, recently, the I_{Kr}-specific blocker dofetilide was approved for treatment of atrial fibrillation (AF) (6). Therefore, the action of I_{Kr} blockers on atrial, as well as ventricular, APs is of interest. The aims of this study were *1*) to establish a human atrial AP model that can differentiate the effects of drugs with the three distinct I_{Kr} blockade kinetics, *2*) to elucidate the underlying mechanism of the different effect of I_{Kr} blockade on APD prolongation, and *3*) to predict the requirement for non-reverse-frequency-dependent prolongation of APD in I_{Kr} blockade. To examine the effects of pure I_{Kr} blockade on APD, other possible effects by the I_{Kr} blockers [e.g., blockade of

Address for reprint requests and other correspondence: Y. Kurachi, Div. of Molecular and Cellular Pharmacology, Dept. of Pharmacology, Graduate School of Medicine, Osaka Univ., 2-2 Yamada-oka, Suita, Osaka 565-0871, Japan (e-mail: ykurachi@pharma2.med.osaka-u.ac.jp).

The costs of publication of this article were defrayed in part by the payment of page charges. The article must therefore be hereby marked "*advertisement*" in accordance with 18 U.S.C. Section 1734 solely to indicate this fact.

ultrarapid delayed rectifier K^+ current (I_{Kur}) and inactivating transient outward K^+ current (I_{to}) by quinidine] needed to be excluded. This is very difficult, if not impossible, in vitro. However, in silico approaches can realize such hypothetical experimental conditions. Therefore, we have developed an applicable human atrial AP model.

We first examined the effect of I_{Kr} blockade caused by dofetilide on the model of human atrial AP that was developed by Courtemanche et al. (2). We found that this model could not reproduce dofetilide's reverse-frequency-dependent prolongation of atrial APD. To correct this defect, we incorporated the slow component of I_{Ks} (27, 31) into the model. The modified model reproduced and accounted for the different frequency-dependent responses of APD due to three kinetically distinctive I_{Kr} blockade types. These results suggest that the voltage and time dependence of I_{Kr} blockade by drugs may be critical for the phenotype of drug effect on atrial AP.

MATERIALS AND METHODS

AP simulation. To simulate the human atrial AP, we used the mathematical model developed by Courtemanche et al. (2). Briefly, this model has passive properties (e.g., membrane capacitance and membrane resistance) and 12 voltage-dependent and carrier-mediated ionic currents as follows: fast Na^+ current (I_{Na}), inward rectifier K^+ current (I_{K1}), I_{to}, I_{Kur}, I_{Kr}, I_{Ks}, L-type Ca^{2+} current ($I_{Ca,L}$), sarcolemmal Ca^{2+} pump current ($I_{p,Ca}$), Na^+-K^+ pump current (I_{NaK}), Na^+/Ca^{2+} exchanger current (I_{NaCa}), background Na^+ current ($I_{b,Na}$), and background Ca^{2+} current ($I_{b,Ca}$). Hodgkin-Huxley-type equations are used to calculate the forward and backward kinetics of the activation and inactivation processes of each voltage-gated ion channel. The program was coded in C/C++, and simulations were run on an IBM-compatible computer with a C++ compiler.

I_{Ks} in the original atrial AP model of Courtemanche et al. (2) is expressed as follows

$$I_{Ks} = g_{Ks} x_s^2 (V - E_K) \quad (1)$$

where g_{Ks} is the maximum conductance for I_{Ks}, x_s is the activation gate variable for I_{Ks}, V is the membrane potential, and E_K is the equilibrium potential for K^+. The activation of I_{Ks} in the original model of Courtemanche et al. is assumed to have one gate represented by squared variables (x_s^2). It has been experimentally shown, however, that I_{Ks} possesses at least two (fast and slow) activation processes (27, 31). The time constant in the original model of Courtemanche et al. represents only the fast process. An additional slow activation process was introduced into the formulation of I_{Ks} in our model in a manner similar to that in the Luo-Rudy (LRd) model, the de facto standard guinea pig ventricle cell model (35). We modified this to incorporate two activation processes as follows

$$I_{Ks} = g_{Ks} x_{s1} x_{s2} (V - E_K) \quad (2)$$

where x_{s1} and x_{s2} are the fast and slow activation gate variables, respectively. Although the time constant of x_{s1} [$\tau_{x(s1)}$] was set to be the same as the value of the time constant of x_s in the original model of Courtemanche et al., that of x_{s2} [$\tau_{x(s2)}$] was two, four, or six times $\tau_{x(s1)}$. The maximum I_{Ks} conductance was adjusted in each case so that the APD in the control at 1,000-ms cycle length (CL) did not change from that of the original model: it was 0.129, 0.187, 0.251, and 0.277 mS/μF for the original and the two-, four-, and sixfold increases, respectively.

Thirty AP simulations were run at each CL. The last AP in each run was used for analysis. The APD was measured at −70 mV, which closely approximates APD at 90% repolarization (APD_{90}).

Formulation of kinetic properties of I_{Kr} blockade types. To incorporate the effects of the three blockade groups, we modified the formulation of I_{Kr} given by Courtemanche et al. (2) as follows

$$I_{Kr} = \frac{y_i g_{K_r} x_r (V - E_K)}{1 + \exp\left(\frac{V + 15}{22.4}\right)} \quad (3)$$

where i represents the blockade type where dofetilide type is the voltage- and time-independent blockade, quinidine type is the voltage-dependent blockade with fast development, and vesnarinone type is the voltage-dependent blockade with slow development, y_i is the fraction of I_{Kr} that is not blocked by drug type i, g_{Kr} is the maximum conductance of I_{Kr}, and x_r is the activation gate variable,.

Dofetilide blocks I_{Kr} in a voltage- and time-independent manner (33). Therefore, dofetilide represents the voltage- and time-independent blockade and $y_{\text{dofetilide type}}$ was set to 0.1.

On the other hand, the effects of the two types of voltage- and time-dependent blockade were calculated with the following first-order differential equation

$$dy_i/dt = (y_{\infty,i} - y_i)/\tau_i \quad (4)$$

where i represents the blockade type where quinidine or vesnarinone, y_i is the state variable of the unblocked fraction of I_{Kr} in the presence of drug type i, $y_{\infty,i}$, is the steady-state value of y_i, and τ_i is the time constant for y_i. Simulations of $y_{\infty,i}$ and τ_i derived from our experimental data for quinidine and dofetilide (33) and vesnarinone (13) are shown in Fig. 1.

$y_{\infty,i}$ and τ_i are expressed as functions of V as follows

$$y_{\infty,i} = \frac{\alpha_i}{\alpha_i + \beta_i} \quad (5)$$

$$\tau_i = \frac{1}{\alpha_i + \beta_i} \quad (6)$$

where i represents quinidine type or vesnarinone type

$$\alpha_{\text{quinidine type}} = 0.000611 - \frac{0.000611 - 0.004661}{1 + \exp\left(\frac{V - 18.2}{-10.8}\right)} \quad (7)$$

$$\beta_{\text{quinidine type}} = \frac{0.00456\left(\frac{1}{y_{\text{depolarization, quinidine type}}} - 1\right)}{1 + \exp\left(\frac{V - 8.67}{-12.9}\right)} \quad (8)$$

$$\alpha_{\text{vesnarinone type}} = 0.0005 \quad (9)$$

$$\beta_{\text{vesnarinone type}} = \frac{0.0005\left(\frac{1}{y_{\text{depolarization, vesnarinone type}}} - 1\right)}{1 + \exp\left(\frac{V - 16.5}{-12.6}\right)} \quad (10)$$

$y_{\text{depolarization},i}$ is the limit set for the minimum of unblocked I_{Kr} ($y_{\infty,i}$), which was set to 0.1 for both drug types and corresponds to 90% block, α_i is the unbinding rate constant for drug type i, and β_i is the binding rate constant for drug type i. The values in the formulas for $y_{\infty,\text{quinidine type}}$ and $\tau_{\text{quinidine type}}$ were determined from the experimental data of Tsujimae et al. (33) by nonlinear least-squares fitting. In the same way, the values in the formulas for $y_{\infty,\text{vesnarinone type}}$ and $\tau_{\text{vesnarinone type}}$ were derived from Katayama et al. (13). The experimental data for the temperature sensitivity of I_{Kr} blockade by these drugs are not available. However, because it was reported that the temperature dependence of I_{Kr} blockade is usually not prominent in various drugs (14), we assumed that the temperature difference among these experiments would not largely affect the present model results. Furthermore, in this study, we adopted the kinetics of dofetilide, quinidine, and vesnarinone from our previous experimental results only to represent the three representative types of I_{Kr} blockade by

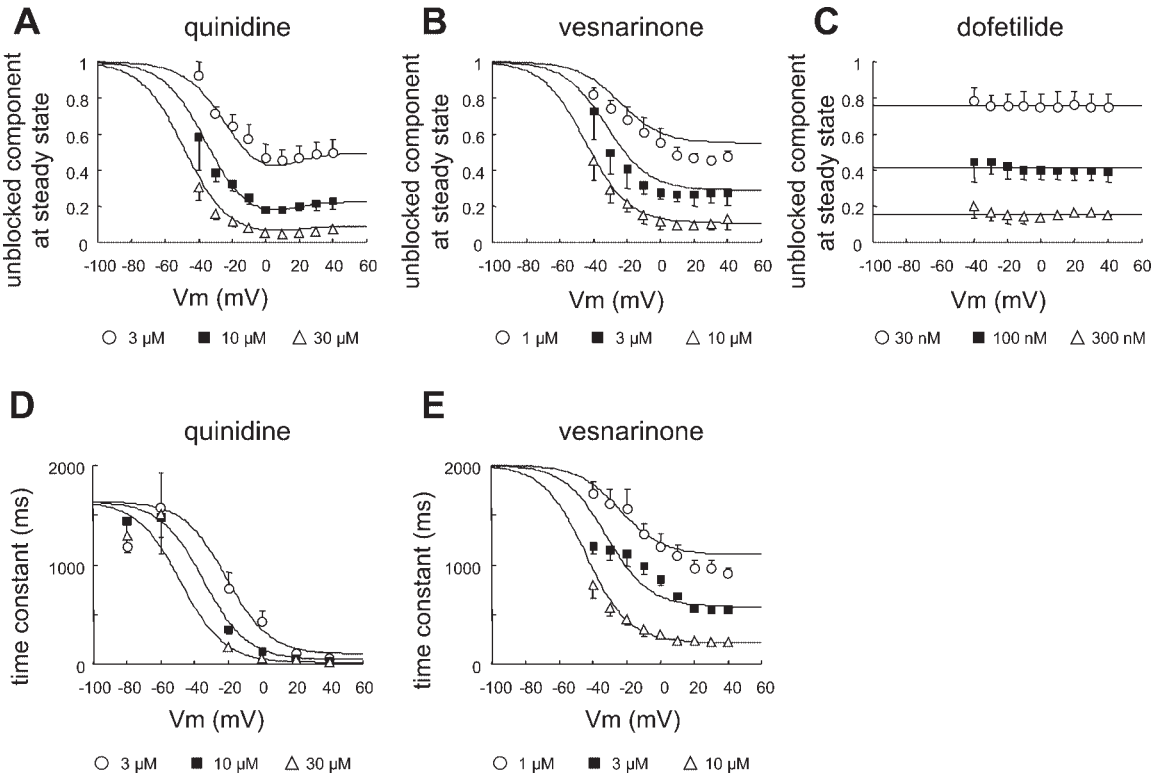

Fig. 1. Modeling of voltage-dependent (*A–C*)- and time-dependent (*D-E*) blockade of I_{Kr} by quinidine (*A* and *D*), vesnarinone (*B* and *E*), and dofetilide (*C*). Traces represent results obtained from formulations of blockade described in MATERIALS AND METHODS. Symbols represent experimental data from Tsujimae et al. (33) for dofetilide and quinidine and from Katayama et al. (13) for vesnarinone. V_m represents membrane potential. Values for $y_{deporalization}$ were 0.159, 0.412, and 0.756 for 30, 100, and 300 nM dofetilide, respectively; 0.491, 0.225, and 0.088 for 3, 10, and 30 μM quinidine, respectively; and 0.550, 0.289, and 0.109 for 1, 3, and 10 μM vesnarinone, respectively.

various drugs, and we did not intend to reproduce precisely the experimental results of the effects of these drugs on atrial AP. These formulations are used to simulate the development and recovery from blockade for dofetilide, quinidine, and vesnarinone (Fig. 2). For simulation of development of blockade, voltage steps (1-s duration) from a holding potential of −80 mV to between −20 and +40 mV with a 20-mV increment (Fig. 2, *A–C*) were used. For simulation of recovery from blockade, voltage steps (10-s duration) from a holding potential of +40 mV to between −40 and −100 mV with a 20-mV increment were used (Fig. 2, *D–F*). Although the kinetics of quinidine blockade are complex and consist of at least two exponential components (33), we treated this as a single-exponential process (Fig. 2, *A* and *D*) (33). Block and recovery due to vesnarinone could be represented by single exponentials (Fig. 2, *B* and *E*) (13). Blockade by dofetilide was constant (Fig. 2, *C* and *F*) (33).

RESULTS

Incorporation of a slow component into I_{Ks} and its effect on APD prolongation caused by reduced I_{Kr} density. We began with the original mathematical model for human atrial AP that had been developed by Courtemanche et al. (2). We first examined the frequency dependence of APD under control conditions and in the presence of a voltage- and time-independent I_{Kr} blocker represented by dofetilide (Fig. 3*A*). The APs exhibit the spike-and-dome morphology commonly observed in human atrial recordings. Several class III antiarrhythmic agents such as dofetilide cause a voltage- and time-independent blockade of I_{Kr} or HERG current (33). The blocking effect of these drugs was termed "dofetilide-type" in the present study and is modeled by reducing the maximum conductance of I_{Kr} to 10% of the control (see MATERIALS AND METHODS). Dofetilide-type 90% blockade of I_{Kr} prolonged the late phase of repolarization at any CL but left AP amplitude and the resting potential unchanged (Fig. 3*A*). This effect is consistent with the experimental data for dofetilide and E-4031 (12, 18). The effect of CL on APD under control conditions and with 90% blockade of I_{Kr} is shown in Fig. 3*Ca*. In control conditions, APD slightly increased when CL was increased from 500 to 700 ms, and APD reached a plateau value of ~300 ms at >800-ms CL. This frequency dependence of the original model correctly captured the feature of the experimental result in the control condition (8). However, when the maximum I_{Kr} conductance was reduced to 10% of control to simulate the voltage- and time-independent blockade, $APD_{-70\ mV}$ was prolonged at all CLs and the CL-dependent increase of APD reached a plateau value of ~400 ms at ~1,000-ms CL. Previous experimental results showed reverse-frequency-dependent prolongation of APD in the atrium at 1,500-ms CL in guinea pig with dofetilide (18) and also in humans with quinidine and flecainide (10). Therefore, the plateau at 1,000-ms CL in the original model is not consistent with the most likely estimation that the reverse-frequency-dependent APD prolongation may also be observed at up to 1,500-ms CL in the human atrium with dofetilide. When APD prolongation was normalized to 500-ms CL, dofetilide-type inhibition of I_{Kr} (Fig. 3*Cc*) clearly demonstrated a CL-dependent increase of $APD_{-70\ mV}$ only at <1,000-ms CL.

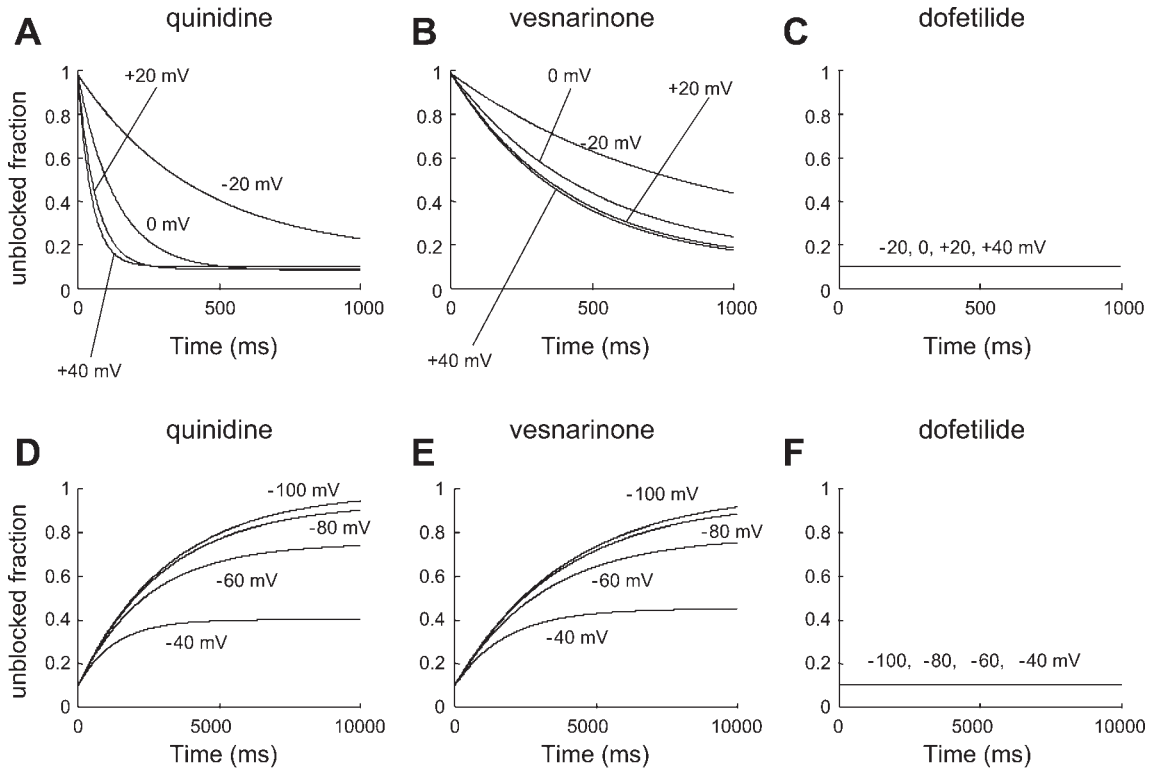

Fig. 2. Simulation of onset and recovery from blockade of I_{Kr} by each drug type. *A–C*: simulation of onset of quinidine-, vesnarinone-, and dofetilide-type I_{Kr} blockade during 1,000-ms voltage steps from −80 to −20, 0, +20, and +40 mV. *D–F*: simulation of recovery from quinidine-, vesnarinone-, and dofetilide-type I_{Kr} blockade during 10,000-ms voltage steps from +40 to −40, −60, −80, and −100 mV. Value for $y_{depolarization}$ was set to 0.1 for each drug type.

The repolarization current for AP in cardiac myocytes is mainly composed of I_{Kr} and I_{Ks}. As shown by Jurkiewicz and Sanguinetti (12) in guinea pig ventricular myocytes, although the magnitude of I_{Kr} activated during depolarizing pulses remains nearly constant at different CLs because of its quick activation, that of I_{Ks} becomes larger as the stimulation rate is increased. As a result, the effect of I_{Kr} blockade on AP is relatively small at fast stimulation rate, where the I_{Ks} is enhanced. It is thus widely accepted that the different level of activation of I_{Ks} at different CLs is the major cause of the reverse-frequency-dependent nature of APD under blockade of I_{Kr}. Therefore, we examined the possibility that inappropriate modeling of I_{Ks} activation/deactivation may account for the failure of the original model of Courtemanche et al. (2) to reproduce the phenomenon.

Activation of I_{Ks} contains fast and slow processes (27, 31). I_{Ks} in the model of Courtemanche et al. (2) has one fast activation process. Therefore, we incorporated a second variable for slow kinetics (x_{s2}) into the activation gate of I_{Ks} (*Eq. 2*). The time constant of slow activation of I_{Ks} has been reported to be three to five times larger than that of fast activation (31). Therefore, we set the slow time constant [$\tau_{x(s2)}$] to two, four, or six times $\tau_{x(s1)}$ (Fig. 4). For each value of $\tau_{x(s2)}$, the maximum conductance of I_{Ks} was adjusted to maintain the AP configuration at 1,000-ms CL.

In Fig. 3*B*, the modified model with I_{Ks} and $\tau_{x(s2)}$ six times $\tau_{x(s1)}$ is used to simulate APs at various CLs. The modified model exhibits a spike-and-dome morphology similar to the original model of Courtemanche et al. (2). At 500-ms CL, APD of the modified model was slightly shorter than APD of the original model, but at 1,000- and 1,500-ms CL, APDs of the modified model were nearly the same as APD of the original model. When I_{Kr} was reduced to 10% of the control to simulate the voltage- and time-independent blockade, the prolongation of APD with longer CL was more prominent in the modified model.

The effect of varying $\tau_{x(s2)}$ on CL-dependent prolongation of $APD_{-70\ mV}$ in the presence of the voltage- and time-independent blocker is shown in Fig. 3*Cb*. In control conditions, as $\tau_{x(s2)}$ increased, $APD_{-70\ mV}$ at 500-ms CL decreased, but $\tau_{x(s2)}$ had less effect at ≥1,000-ms CL. When I_{Kr} was reduced as $\tau_{x(s2)}$ was increased, CL-dependent prolongation of $APD_{-70\ mV}$ was more apparent, and the slope of the CL-$APD_{-70\ mV}$ relation became steeper. When $\tau_{x(s2)}$ was set to four or six times $\tau_{x(s1)}$, $APD_{-70\ mV}$ did not reach a plateau until 1,500-ms CL. In addition, normalization of $APD_{-70\ mV}$ prolongation caused by reduced I_{Kr} density (Fig. 3*Cc*) clearly demonstrated that the prolongation of $APD_{-70\ mV}$ caused by I_{Kr} reduction depends on $\tau_{x(s2)}$. Clearly, these results more closely resemble experimental results (12, 18) than those obtained with the original model of Courtemanche et al. (2) (Fig. 3*Ca*). Therefore, in the following studies, we used the modified model with $\tau_{x(s2)}$ set to six times $\tau_{x(s1)}$.

Comparison of delayed rectifier currents in original and modified models. Figure 5 shows I_{Kr} and I_{Ks} during APs at various CLs in the original and modified models. Since the formulation of I_{Kr} was not modified, the form and amplitude of I_{Kr} during each AP at each CL in the original (Fig. 5*A*) and modified (Fig. 5*B*) models were very similar. The peak of I_{Kr} during an AP increased as APD was prolonged, because the

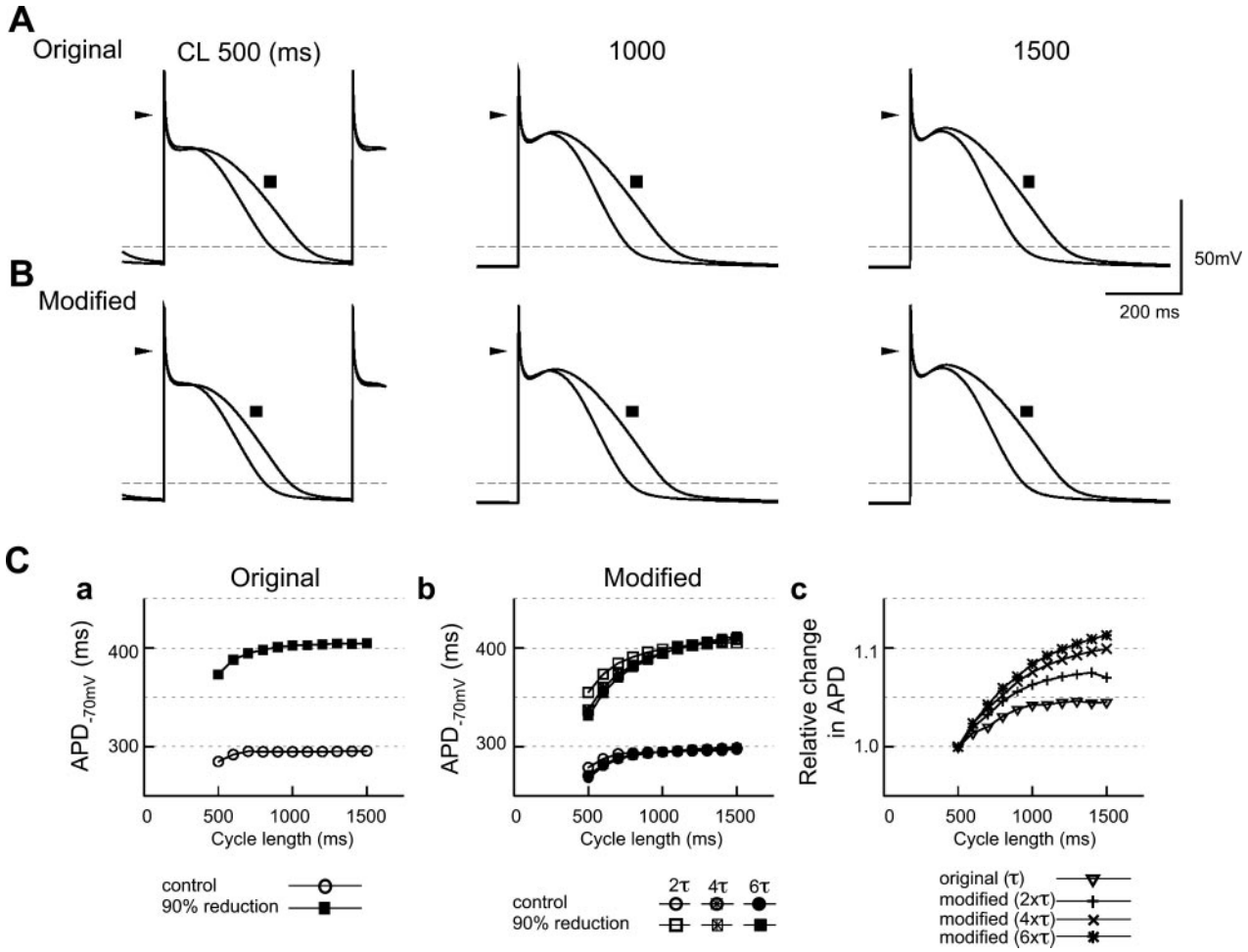

Fig. 3. Frequency-dependent effects of 90% reduction in rapidly activating K^+ current (I_{Kr}) density on prolongation of action potential (AP) duration (APD) in models of human atrial AP. *A*: simulated APs with the original model of Courtemanche et al. (2) at 500-, 1,000-, and 1,500-ms cycle length (CL). Simulations correspond to control conditions and 90% reduction of maximum I_{Kr} conductance (filled square). *B*: same as *A*, with a modified model, where a slow component (x_{s2}) is added to the activation gate of I_{Ks} (*Eq. 2*). Time constant of x_{s2} was 6 times that of x_{s1}. *Ca*: $APD_{-70\,mV}$-CL relation with the original model of Courtemanche et al. under control conditions and after 90% reduction of maximum I_{Kr} conductance. *Cb*: effects of alteration of time constant of slow component of activation of slowly activating K^+ current (I_{Ks}, x_{s2}) in the modified model on CL-APD relation under control conditions and after 90% reduction of I_{Kr}. Slow time constants 2, 4, and 6 times the time constant of the fast component of I_{Ks} (x_{s1}) were tested. *Cc*: effect of CL on $APD_{-70\,mV}$ prolongation after 90% reduction of maximum I_{Kr} conductance in original and modified models. Values were normalized to 500-ms CL. Modified model involved inclusion of a slow phase of activation of I_{Ks} (x_{s2}) with time constants of activation 2, 4, and 6 times the time constant of x_{s1}.

activation process of I_{Kr} progressed during an AP, even in the presence of very rapid C-type inactivation (36). As CL increased, I_{Kr} increased by the same amount in both models, although at 500-ms CL, the peak of I_{Kr} was slightly smaller during an AP in the modified than in the original model.

In the original model, I_{Ks} increased as CL increased, similar to I_{Kr} (Fig. 5*A*). On the other hand, in the modified model, I_{Ks} decreased as CL increased (Fig. 5*B*), which is consistent with the experimental results shown by Jurkiewicz and Sanguinetti (12). Analysis of the gating variables (gate in Fig. 5) indicates that the difference in the behavior of I_{Ks} in the two models may be attributed mainly to the properties of x_{s2}. Because its time constant was slow, x_{s2} showed only slight variation during an AP: it increased slowly during depolarization and declined slowly during repolarization (Fig. 5*B* gate, thick continuous line). At 500-ms CL, x_{s2} at the onset of an AP was high and decreased as CL was prolonged to 1,000 and 1,500 ms. In contrast, the fast gating variables, x_s in the original model (Fig. 5*A*) and x_{s1} in the modified model (Fig. 5*B* gate, thin line), increased rapidly during depolarization and decreased rapidly during repolarization.

As a result of these differences, deactivation of the product of x_{s1} and x_{s2} in *Eq. 2* for the modified model is slower than deactivation of x_s^2 in *Eq. 1* in the original model. Consequently, at short CL in the modified model, I_{Ks} showed little deactivation at the end of repolarization, and its initial jump at the onset of the next AP was large; with increasing CL, deactivation could develop further, and the amplitude of the initial jump decreased markedly. After the initial jump, I_{Ks} increased during an AP, but the combination of a slower activation and the decline of the initial current meant that the peak of I_{Ks} during an AP decreased as CL was prolonged. On the other hand, in the original model, deactivation was more rapid, and the initial jump of I_{Ks} was less at 500-ms CL and was influenced less by increasing CL. I_{Ks} increased rapidly during an AP because of its fast activation kinetics, and peak I_{Ks} increased with CL.

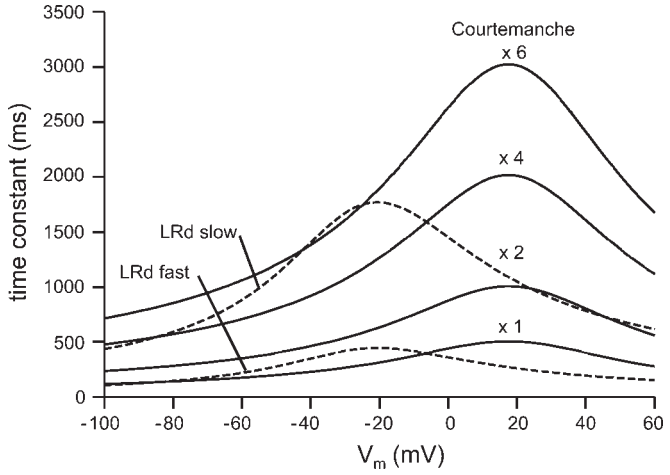

Fig. 4. Comparison of voltage dependence of time constants of activation gate of I_{Ks} described by Courtemanche et al. (2) and the two gates of I_{Ks} (LRd fast and LRd slow) used in the Luo-Rudy ventricular AP model (35). Equivalent of the time constant of the model of Courtemanche et al. (2) multiplied by 2, 4, and 6, which we used as time constants for the slow gating component (x_{s2}) of I_{Ks}, is also shown.

Finally, in the original model, the relative proportions of I_{Kr} and I_{Ks} showed little change with CL [Fig. 5*A*; $I_{Kr}/(I_{Kr} + I_{Ks})$]. In the modified model, the contribution of I_{Kr} to the total repolarizing current increased with CL (Fig. 5*B*). Thus it is the modified model that can reproduce the experimental data for the frequency-dependent behavior of I_{Ks} and APD.

Effects of I_{Kr} blockers on APD prolongation. Experimentally, it is also recognized that excessive AP prolongation is quite divergent among dofetilide, quinidine, and vesnarinone (10, 12, 32). We next examined how voltage- and time-dependent kinetics in I_{Kr} blockade affect the reverse frequency dependence of APD prolongation in the model. Although dofetilide and E-4031 block I_{Kr} in a voltage-independent manner, quinidine and vesnarinone do so in a voltage- and time-dependent manner (13, 33). Both drugs inhibit the current more potently and rapidly as the membrane potential is more depolarized. However, at the same depolarized potential, the development of block is much faster with quinidine than with vesnarinone. To isolate the effects of these three typical kinetic properties of I_{Kr} blockade, we fixed their maximal effect to correspond to 90% block of I_{Kr}. Thus we calibrated the blockades with different kinetics by assuming the same possible maximal block effect, so that the effects of the kinetics of I_{Kr} blockade on APD can be compared selectively. This is represented in the calculations as a steady-state unblocked fraction of 0.1 (see MATERIALS AND METHODS).

Figure 6 illustrates the effects of these drug types on APD at different CLs in absolute and relative terms. Dofetilide-type blockade exhibited the strongest and the most prominent reverse-frequency-dependent increase in $APD_{-70\,mV}$ (Fig. 6*A*). Quinidine-type blockade was less effective than dofetilide-type

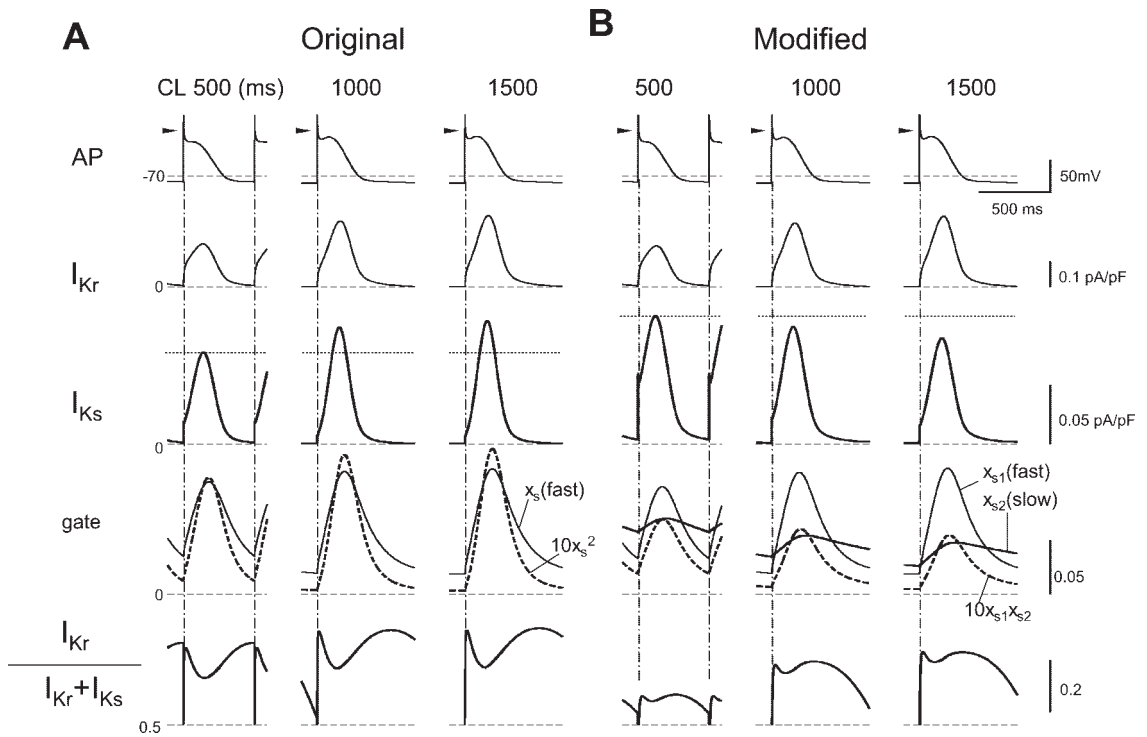

Fig. 5. Contributions of I_{Kr} and I_{Ks} to AP simulated by different models and at different CLs. *A* and *B*: simulations with original model of Courtemanche et al. (2) and modified model at 500-, 1,000-, and 1,500-ms CL. AP: representative APs. Arrowheads, 0 mV. I_{Kr} and I_{Ks}: time course of simulations of I_{Kr} and I_{Ks} currents during APs. Dashed horizontal lines (I_{Kr} and I_{Ks}) indicate 0 pA/pF; dotted horizontal lines (I_{Ks}) indicate maximum current through I_{Ks} during AP at 500-ms CL. Gate: time course of gating variables (x_s in *A* and x_{s1} and x_{s2} in *B*) of I_{Ks}. To facilitate comparison between gating of I_{Ks} in *A* and *B*, dashed lines represent the product of the gating variables: x_s^2 in *A* and x_{s1} and x_{s2} in *B*. Data have been multiplied by 10 to appear on this scale. $I_K/(I_{Kr} + I_{Ks})$: contribution of I_{Kr} to total I_K during each AP.

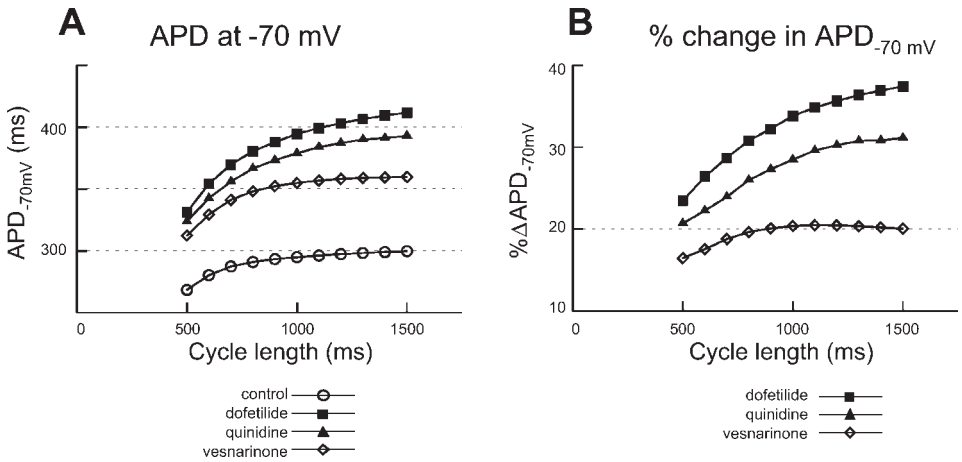

Fig. 6. AP elongation by blockade of I_{Kr} from modified model. *A*: effect of CL on APD (measured at −70 mV) under control conditions and in the presence of dofetilide, quinidine, or vesnarinone. *B*: data from *A* normalized as drug-induced increase in APD relative to APD under control conditions.

blockade but showed a similar reverse frequency dependence. Vesnarinone-type blockade was weaker than quinidine- or dofetilide-type blockade, and it showed no frequency dependence at >800-ms CL. The result in relative terms also more clearly demonstrates no frequency dependence of vesnarinone-type blockade at >800-ms CL; thus frequency dependence is similar for vesnarinone-type blockade and control (Fig. 6*B*). These results are consistent with experimental findings (10, 12, 32). We conclude that the modified model can reproduce the characteristic frequency-dependent prolongation of atrial APD by the I_{Kr} blockers with the three representative kinetics.

Figure 7 shows the effects of the three drugs on AP configuration and the two delayed rectifier currents I_{Kr} and I_{Ks}. At 500-, 1,000-, and 1,500-ms CL, all three drug types significantly prolonged AP without affecting the AP amplitude and the resting potential (Fig. 7). With increasing CL, quinidine- and dofetilide-type blockade progressively prolongs APD to a similar extent, whereas vesnarinone-type blockade became less effective (see also Fig. 6*B*).

To determine the mechanisms underlying these different effects, the unblocked fractions of I_{Kr} (y_i), the total amount of repolarization current ($I_{Kr} + I_{Ks}$), and the contribution of I_{Kr} to the repolarization current [$I_{Kr}/(I_{Kr} + I_{Ks})$] were examined (Fig. 7). The dofetilide-type blocking effect ($y_{\text{dofetilide type}}$) was constant and independent of CL (Fig. 4, unblocked fraction). Vesnarinone- and quinidine-type drugs cause voltage- and time-dependent blockade of I_{Kr} (Figs. 1 and 2), with blockade during depolarization and recovery during repolarization. The corresponding values for $y_{\text{quinidine type}}$ and $y_{\text{vesnarinone type}}$ decrease with depolarization and increase with recovery (Fig. 7, unblocked fraction). The values for $y_{\text{quinidine type}}$ and $y_{\text{vesnarinone type}}$ are maximal just before each AP. As CL increases, these maximum values for $y_{\text{quinidine type}}$ and $y_{\text{vesnarinone type}}$ increase as the time allowed for unblocking increased. At the onset of an AP, $y_{\text{quinidine type}}$ decreases, and during the AP it reaches a minimum value of ~0.2 irrespective of CL. This shows that, in practical terms, quinidine blocks I_{Kr} in a frequency-independent manner because of its fast blocking kinetics. Therefore, quinidine- and dofetilide-type blockades have functionally similar effects on I_{Kr} during AP, although they have very different kinetics. In contrast, the minimum value of $y_{\text{vesnarinone type}}$ was dependent on CL; that is, maximum blockade of I_{Kr} by vesnarinone was attenuated as CL was prolonged.

The total delayed rectifier current increases with increasing CL under control conditions (Fig. 7, $I_{Kr} + I_{Ks}$) because of the increase in I_{Kr} [Fig. 7, $I_{Kr}/(I_{Kr} + I_{Ks})$; see also Fig. 5*B*, I_{Kr}]. In the presence of a vesnarinone-type drug, total I_K also increased with increasing CL, because the relative proportion of I_{Kr} also increased. As a result, vesnarinone-type blockade did not induce reverse-frequency-dependent prolongation of APD. In contrast, in the presence of dofetilide- and quinidine-type drugs, total I_K decreased as CL was prolonged. This is due to their constant maximum blockade of I_{Kr} over a wide range of CL and the reduction of I_{Ks} with longer CL. As a result, APD prolongation with CL was enhanced by dofetilide- and quinidine-type blockade.

DISCUSSION

The major findings in this study are as follows. *1*) Incorporation of a slow process of activation into I_{Ks} enabled a human atrial AP model to reproduce the reverse-frequency-dependent elongation of APD that is associated with the reduction of I_{Kr}. *2*) This model could account for the mechanisms underlying the difference between the frequency-dependent effects of the three kinetically distinctive types (dofetilide, quinidine, and vesnarinone) of I_{Kr} blockade on APD. *3*) The analysis with the models predicted that the drugs with the voltage- and time-dependent I_{Kr} blockade with slow kinetics may be good candidates without the adverse effect of arrhythmias.

There are many mathematical models for cardiac APs, e.g., models for Purkinje fibers (19, 20), rabbit sinoatrial node (4), and ventricular cells of rat (22, 23), guinea pig (35, 40), dog (9, 38), and human (24) and models for atrial cells of dog (15, 25) and human (2, 21). No model is perfect, but each has its use for examination of different properties of cardiac AP behavior, with their respective limitations taken into account. In practical terms, it is important to adjust models according to the purposes for which they will be used.

A problem in pharmacology is the proarrhythmic action of many drugs. A number of compounds inhibit I_{Kr} in cardiac myocytes and, therefore, have the potential to prolong the AP in a reverse-frequency-dependent manner, which could induce torsades de pointes in the ventricle. Because of this side effect, drugs such as terfenadine, astemizole, grepafloxacin, droperidol, and cisapride have been withdrawn or restricted in their

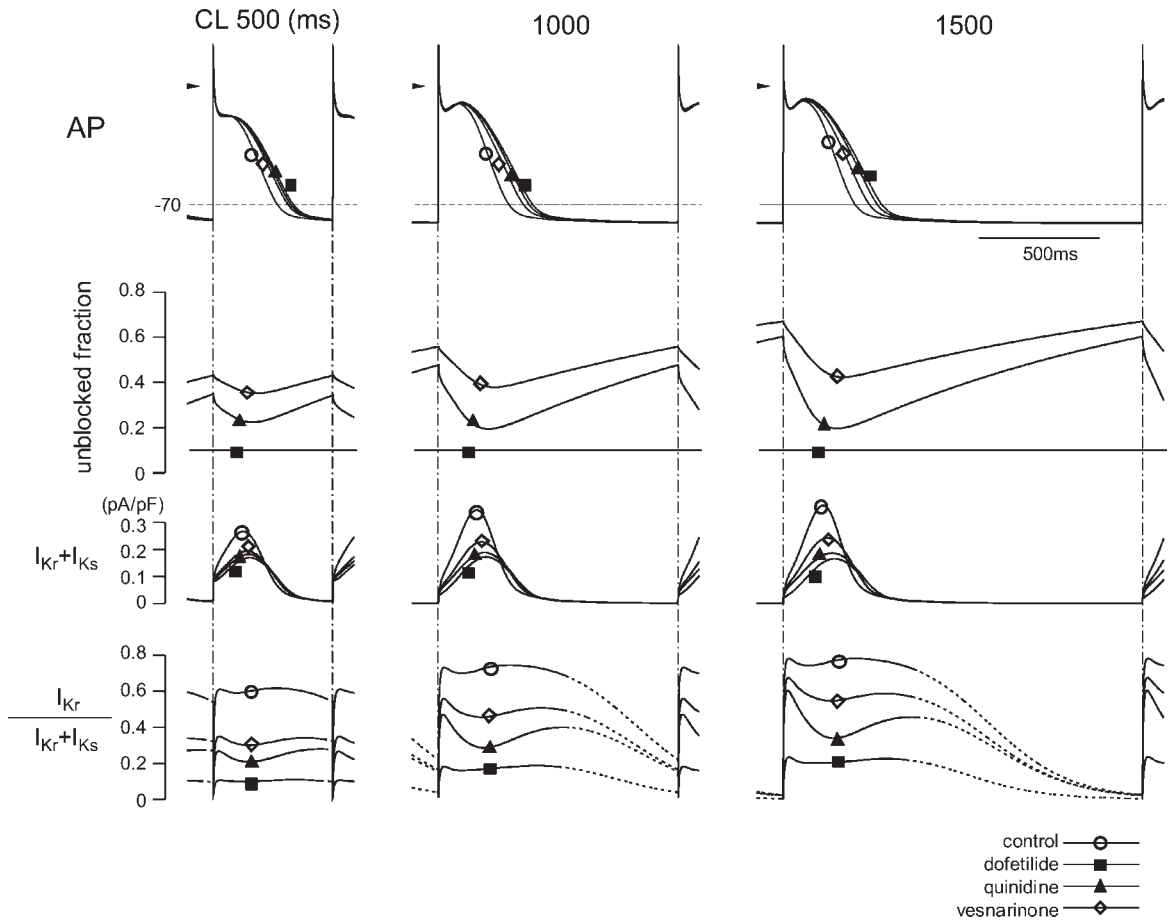

Fig. 7. Effects of I_{Kr} blockade on AP and I_{Kr} and I_{Ks} at 500-, 1,000-, and 1,500-ms CL. AP: simulations of APs at 500-, 1,000-, and 1,500-ms CL under control conditions and in the presence of dofetilide, quinidine, and vesnarinone. Arrowheads, 0 mV. Unblocked fraction: y_i for I_{Kr} for each drug type (see *Eq. 4*). Traces show degree and time course of blockade of I_{Kr} by each drug. $I_{Kr} + I_{Ks}$: total I_K. Traces show time course of these currents during AP at 500-, 1,000-, and 1,5000-ms CL and effects of dofetilide, quinidine, and vesnarinone on I_{Kr} blockade. $I_{Kr}/(I_{Kr} + I_{Ks})$: contribution of I_{Kr} to total I_K.

clinical application (26). Also, the development of a number of new pharmacological agents was stopped when they were shown to block I_{Kr}. A mathematical model of the cardiac AP that can reproduce reverse-frequency-dependent APD prolongation on I_{Kr} blockade could be used to assess the risk of such side effects.

Inasmuch as dofetilide has been approved by the US Food and Drug Administration for treatment of AF (6), the importance of elucidating the action of I_{Kr} blockade on atrial APD prolongation is increasing. The model of the human atrial AP of Courtemanche et al. (2) could not reproduce reverse-frequency-dependent elongation of APD with blockade of I_{Kr}. To reproduce this property, we introduced a slow process of activation and deactivation of I_{Ks}, which has been identified experimentally (27, 31). The modified human atrial AP model reproduced reverse-frequency-dependent prolongation of atrial APD, which results from the reduction of maximum conductance of I_{Kr} by voltage- and time-independent I_{Kr} blockers such as dofetilide and E-4031. It also differentiates between the effects of the voltage- and time-dependent blockade caused by quinidine- and vesnarinone-type I_{Kr} blockers. Therefore, the model can be used to assess the frequency-dependent action of different types of pure I_{Kr} blockade on the human atrial AP. Because the simulation results with pure I_{Kr} blockade are very close to the experimental results of the effects of dofetilide, quinidine, and vesnarinone on atrial APD (10, 18, 32), it was also suggested that the effects of these drugs on I_{Kr} are the major determinants for atrial APD, although quinidine is known to affect a number of ion currents, including I_{Na} and I_{to}, and vesnarinone is known to increase $I_{Ca,L}$ (16, 39). Indeed, our preliminary model study showed that additional blockade of I_{Kur} and I_{to} only marginally enhanced the reverse frequency dependence of APD prolongation induced purely by the quinidine-type blockade of I_{Kr} (not shown).

This study showed that the slow activation/deactivation of I_{Ks} plays an important role in reproducing the reverse-frequency-dependent APD prolongation by I_{Kr} blockers in an atrial model. The Luo-Rudy model (35, 40), which is the de facto standard for the guinea pig ventricular cell, also has fast and slow components of I_{Ks} activation; in this example, the slow time constant is four times the fast (35) (Fig. 4). Reconstitution of I_{Ks} with KvLQT1/minK exhibited three activation processes: fast, slow, and very slow (27). The time constants for fast and slow were 0.68 and 1.48 s, respectively, at +40 mV, which approximate the fast and slow activation processes of I_{Ks} that we use. We have not incorporated the very slow time constant (8.0 s at +40 mV) into I_{Ks}. If this slower activation process were incorporated into our model, the reverse-frequency-dependent APD prolon-

gation associated with the dofetilide-type of blockade of I_{Kr} would become more prominent. Further experimental studies are needed to identify the gating processes of I_{Ks} for further improvement of the model.

APD is shorter in atrial cells from AF patients than from normal subjects; this is due to electrical remodeling of atrial myocytes, where expression of ion channel currents, including $I_{Ca,L}$, I_{to}, I_{Kur}, and I_{K1}, is altered (5). Courtemanche and colleagues (3) incorporated such changes into their original model and examined the effects of modification of the different outward currents on atrial AP configuration. The modified human atrial AP model that we present here could also be extended to an AF-atrial AP model that will be suitable for assessing the effects of drugs with the potential to treat AF.

In conclusion, this simulation showed that slow activation and deactivation of I_{Ks} underlie the reverse-frequency-dependent atrial APD prolongation induced by I_{Kr} blockers. It also demonstrated that the effects of these compound types on APD prolongation depended on the kinetics of their interactions with I_{Kr}. Further studies may provide useful information for understanding the underlying mechanisms of cardiac arrhythmias and estimating the balance between antiarrhythmic effect and proarrhythmic risk of I_{Kr} blocking agents. This approach may also be useful for the in silico design of antiarrhythmic agents.

ACKNOWLEDGMENTS

We thank Dr. I. Findlay and A. O'Meara for comments about the manuscript.

GRANTS

This work was supported by the Leading Project for Biosimulation "Development of Heart and Lung Models for In Silico Prediction of Drug Action and Clinical Treatment" from the Ministry of Education, Culture, Sports, Science, and Technology (Japan) to Y. Kurachi.

REFERENCES

1. **Belardinelli L, Antzelevitch C, Vos MA.** Assessing predictors of drug-induced torsade de pointes. *Trends Pharmacol Sci* 24: 619–625, 2003.
2. **Courtemanche M, Ramirez RJ, Nattel S.** Ionic mechanisms underlying human atrial action potential properties: insights from a mathematical model. *Am J Physiol Heart Circ Physiol* 275: H301–H321, 1998.
3. **Courtemanche M, Ramirez RJ, Nattel S.** Ionic targets for drug therapy and atrial fibrillation-induced electrical remodeling: insights from a mathematical model. *Cardiovasc Res* 42: 477–489, 1999.
4. **Demir SS, Clark JW, Murphey CR, Giles WR.** A mathematical model of a rabbit sinoatrial node cell. *Am J Physiol Cell Physiol* 266: C832–C852, 1994.
5. **Dobrev D, Ravens U.** Remodeling of cardiomyocyte ion channels in human atrial fibrillation. *Basic Res Cardiol* 98: 137–148, 2003.
6. **Elming H, Brendorp B, Pedersen OD, Kober L, Torp-Petersen C.** Dofetilide: a new drug to control cardiac arrhythmia. *Expert Opin Pharmacother* 4: 973–985, 2003.
7. **Feldman AM, Baughman KL, Lee WK, Gottlieb SH, Weiss JL, Becker LC, Strobeck JE.** Usefulness of OPC-8212, a quinolinone derivative, for chronic congestive heart failure in patients with ischemic heart disease or idiopathic dilated cardiomyopathy. *Am J Cardiol* 68: 1203–1210, 1991.
8. **Fermini B, Wang Z, Duan D, Nattel S.** Differences in rate dependence of transient outward current in rabbit and human atrium. *Am J Physiol Heart Circ Physiol* 263: H1747–H1754, 1992.
9. **Greenstein JL, Wu R, Po S, Tomaselli GT, Winslow RL.** Role of the calcium-independent outward current I_{to1} in shaping action potential morphology and duration. *Circ Res* 87: 1026–1033, 2000.
10. **Hatem S, Le Grand B, Le Heuzey JY, Couetil JP, Deroubaix E.** Differential effects of quinidine and flecainide on plateau duration of human atrial action potential. *Basic Res Cardiol* 87: 600–609, 1992.
11. **Hondeghem LM, Snyders DJ.** Class III antiarrhythmic agents have a lot of potential but a long way to go. Reduced effectiveness and dangers of reverse use dependence. *Circulation* 81: 686–690, 1990.
12. **Jurkiewicz NK, Sanguinetti MC.** Rate-dependent prolongation of cardiac action potentials by a methanesulfonanilide class III antiarrhythmic agent. Specific block of rapidly activating delayed rectifier K^+ current by dofetilide. *Circ Res* 72: 75–83, 1993.
13. **Katayama Y, Fujita A, Ohe T, Findlay I, Kurachi Y.** Inhibitory effects of vesnarinone on cloned cardiac delayed rectifier K^+ channels expressed in a mammalian cell line. *J Pharmacol Exp Ther* 294: 339–346, 2000.
14. **Kirsch GE, Trepakova ES, Brimecombe JC, Sidach SS, Erickson HD, Kochan MC, Shyjka LM, Lacerda AE, Brown AM.** Variability in the measurement of hERG potassium channel inhibition: effects of temperature and stimulus pattern. *J Pharmacol Toxicol Methods* 50: 93–101, 2004.
15. **Kneller J, Ramirez RJ, Chartier D, Courtemanche M, Nattel S.** Time-dependent transients in an ionically based mathematical model of the canine atrial action potential. *Am J Physiol Heart Circ Physiol* 282: H1437–H1451, 2002.
16. **Lathrop DA, Nanasi PP, Schwartz A, Varro A.** Ionic basis for OPC-8212-induced increase in action potential duration in isolated rabbit, guinea pig and human ventricular myocytes. *Eur J Pharmacol* 240: 127–137, 1993.
17. **Martin CL, Palomo MA, McMahon EG.** Comparison of bidisomide, flecainide and dofetilide on action potential duration in isolated canine atria: effect of isoproterenol. *J Pharmacol Exp Ther* 278: 154–162, 1996.
18. **Matsuda T, Takeda K, Ito M, Yamagishi R, Tamura M, Nakamura H, Tsuruoka N, Saito T, Masumiya H, Suzuki T, Iida-Tanaka N, Itokawa-Matsuda M, Yamashita T, Tsuruzoe N, Tanaka H, Shigenobu K.** Atria selective prolongation by NIP-142, an antiarrhythmic agent, of refractory period and action potential duration in guinea pig myocardium. *J Pharm Sci* 98: 33–40, 2005.
19. **McAllister RE, Noble D, Tsien RW.** Reconstruction of the electrical activity of cardiac Purkinje fibres. *J Physiol* 251: 1–59, 1975.
20. **Noble D.** A modification of the Hodgkin-Huxley equations applicable to Purkinje fibre action and pace-maker potentials. *J Physiol* 160: 317–352, 1962.
21. **Nygren A, Fiset C, Firek L, Clark JW, Lindblad DS, Clark RB, Giles WR.** Mathematical model of an adult human atrial cell: the role of K^+ currents in repolarization. *Circ Res* 82: 63–81, 1998.
22. **Pandit SV, Clark RB, Giles WR, Demir SS.** A mathematical model of action potential heterogeneity in adult rat left ventricular myocytes. *Biophys J* 81: 3029–3051, 2001.
23. **Pandit SV, Giles WR, Demir SS.** A mathematical model of the electrophysiological alterations in rat ventricular myocytes in type-I diabetes. *Biophys J* 84: 832–841, 2003.
24. **Priebe L, Beuckelmann DJ.** Simulation study of cellular electric properties in heart failure. *Circ Res* 82: 1206–1223, 1998.
25. **Ramirez RJ, Nattel S, Courtemanche M.** Mathematical analysis of canine atrial action potential. *Am J Physiol Heart Circ Physiol* 279: H1767–H1785, 2000.
26. **Roden DM.** Drug-induced prolongation of the QT interval. *N Engl J Med* 350: 1013–1022, 2004.
27. **Sanguinetti MC, Curran ME, Zou A, Shen J, Spector PS, Atkinson DL, Keating MT.** Coassembly of K_VLQT1 and minK(IsK) proteins to form cardiac I_{Ks} potassium channel. *Nature* 384: 80–83, 1996.
28. **Sanguinetti MC, Jurkiewicz NK.** Two components of cardiac delayed rectifier K^+ current. Differential sensitivity to block by class III antiarrhythmic agents. *J Gen Physiol* 96: 195–215, 1990.
29. **Sanguinetti MC, Jurkiewicz NK.** Delayed rectifier outward K^+ current is composed of two currents in guinea pig atrial cells. *Am J Physiol Heart Circ Physiol* 260: H393–H399, 1991.
30. **Smith WM, Gallagher JJ.** "Les torsades de pointes": an unusual ventricular arrhythmia. *Ann Intern Med* 93: 578–584, 1980.
31. **Tohse N.** Calcium-sensitive delayed rectifier potassium current in guinea pig ventricular cells. *Am J Physiol Heart Circ Physiol* 258: H1200–H1207, 1990.
32. **Toyama J, Kamiya K, Cheng J, Lee JK, Suzuki R, Kodama I.** Vesnarinone prolongs action potential duration without reverse frequency dependence in rabbit ventricular muscle by blocking the delayed rectifier K^+ current. *Circulation* 96: 3696–3703, 1997.

33. **Tsujimae K, Suzuki S, Yamada M, Kurachi Y.** Comparison of kinetic properties of quinidine and dofetilide block of HERG channels. *Eur J Pharmacol* 493: 29–40, 2004.
34. **Valentin JP, Hoffmann P, De Clerck F, Hammond TG, Hondeghem L.** Review of the predictive value of the Langendorff heart model (Screenit system) in assessing the proarrhythmic potential of drugs. *J Pharmacol Toxicol Methods* 49: 171–181, 2004.
35. **Viswanathan PC, Shaw RM, Rudy Y.** Effects of I_{Kr} and I_{Ks} heterogeneity on action potential duration and its rate dependence: a simulation study. *Circulation* 99: 2466–2474, 1999.
36. **Wang S, Liu S, Morales MJ, Strauss HC, Rasmusson RL.** A quantitative analysis of the activation and inactivation kinetics of HERG expressed in *Xenopus* oocytes. *J Physiol* 502: 45–60, 1997.
37. **Wang Z, Fermini B, Nattel S.** Rapid and slow components of delayed rectifier current in human atrial myocytes. *Cardiovasc Res* 28: 1540–1546, 1994.
38. **Winslow RL, Rice J, Jafri S, Marbán E, O'Rourke B.** Mechanisms of altered excitation-contraction coupling in canine tachycardia-induced heart failure. II. Model studies. *Circ Res* 84: 571–586, 1999.
39. **Yatani A, Imoto Y, Schwartz A, Brown AM.** New positive inotropic agent OPC-8212 modulates single Ca^{2+} channels in ventricular myocytes of guinea pig. *J Cardiovasc Pharmacol* 13: 812–819, 1989.
40. **Zeng J, Laurita KR, Rosenbaum DS, Rudy Y.** Two components of the delayed rectifier K^+ current in ventricular myocytes of the guinea pig type. Theoretical formulation and their role in repolarization. *Circ Res* 77: 140–152, 1995.